

# Passivity-based Control of a PWM operated Digital Hydraulic Drive\*

Helmut Kogler<sup>ℒ</sup>, Markus Schöberl<sup>ℳ</sup> and Rudolf Scheidl<sup>ℳ</sup>

<sup>ℒ</sup>Linz Center of Mechatronics

<sup>ℳ</sup>Johannes Kepler University

Altenberger Strasse 69  
4040 Linz, Austria.  
helmut.kogler@lcm.at

## Abstract

Digital hydraulics offers a cost effective and robust opportunity to replace expensive and sensitive hydraulic servo valves for cylinder drives. If the digital directional valves are operated in pulse width mode at a constant switching frequency the mean flow rate through the valves into the actuator is controlled by the duty ratio of the PWM signal. However, for a proper implementation of digital hydraulic linear drives some adaptations must be made compared to common cylinder drives. In this paper a gas loaded accumulator is used in order to tune the dynamics of the system for a smooth behavior of the drive, which is generally nonlinear. An energy-based controller according to the passivity concept in combination with a load observer is presented. Simulations show the achievable performance.

**Keywords:** digital, hydraulics, switching, passivity, control

## 1 Introduction

In industrial plants often hydraulic actuators are used for the control of heavy mechanical loads due to their invulnerable force density compared to other drive technologies. Furthermore, the simplicity and robustness of linear hydraulic actuators as cylinders, plungers, etc. are outstanding properties of hydraulic drives. On the other hand the mentioned actuators have a nonlinear dynamic behavior, which must be considered in the controller design in order to achieve the desired control performance over a wide operating range. There exist

numerous methods dealing with the control of nonlinear dynamic systems. Well known concepts are, for instance, exact linearization by static feedback, input-output linearization and differential flatness, see e.g. [1, 2]. Unmeasured system states, respectively, unknown loads of flat systems can be estimated with observers, for instance, according to [3]. These concepts have already been successfully applied to hydraulic actuator systems as presented, for instance, in [4, 5, 6, 7]. These mentioned approaches rely on the knowledge of an exact mathematical model according to a physical description of the dynamic behavior of the system. In cases where such a model is not available or difficult to obtain, concepts like sliding mode control or fuzzy control are particularly suitable methods for the controller design, see e.g. [8, 9, 10, 11]. Such concepts have been successfully applied to hydraulic drive systems, like presented in [12, 13, 14]. In [15, 16, 17] an energy-based concept of impedance control is applied to drive systems with hydraulic actuators. Another possibility to deal effectively with nonlinearities of dynamic systems is the passivity based control of Port Hamiltonian Systems as presented, for instance, in [18, 19]. This method gives insight into the flow of energy within the system under investigation and, thus, allows often a pleasing physical interpretation of the resulting control laws.

Today, in hydraulic drive systems the oil flow to the hydraulic actuator is mostly controlled by proportional valves or, in particular, by electro-hydraulic servovalves. In order to achieve a fast and precise proportional valve opening, the servovalves consist at least of one pilot stage and a main stage interconnected with a complicated mechanical or electrical feedback mechanism. For this reason servo valves are expensive components, which are in turn sensitive against oil contamination due to the small clearance of the mechanical valve parts. Furthermore, the resulting requirements on the oil cleanliness lead to additional costs for adequate filtering systems. Moreover, in order to achieve the de-

\*© Proceedings of the IMechE Part I: Journal of Systems and Control Engineering, doi: 10.1177/0959651818806420

sired control accuracy often critically centered spool valves or even valves with negative valve overlap in the closed position are necessary, which result in high piloting and leakage flows and, thus, in high energy consumption even when the drive is not moving.

As an alternative digital hydraulic valves can be used. Basically, digital hydraulics attempts to replace proportional valves by digital valves, see for instance [20, 21, 22, 23]. Digital valves are much simpler in their design, thus, such valves can be produced at lower costs compared to servovalves [24, 25]. Furthermore, since digital valves only have two different switching states and large flow cross-sections they are robust against oil contamination compared to proportional valves. Additionally, in case of seat type valves the leakage flow in closed position can be avoided at all and, thus, the energy consumption of the drive system can be reduced significantly.

Basically, in digital hydraulics there are two different approaches, how proportional valves can be replaced with digital valves; on the one hand according to Fig. 1a with a so called Digital Flow Control Unit (DFCU), for instance, according to [26], which consists of a parallel arrangement of a number of digital valves, possibly, with different nominal flow rates in order to quantize the flow into the cylinder like a hydraulic digital-analogue converter; on the other hand regarding Fig. 1b, where the mean flow can be controlled by fast switching directional digital valves operated in pulse-width-mode (PWM) at a constant switching frequency, as presented in [27].

In this paper a hydraulic drive system controlled with digital valves is presented. For cost reasons the number of valves is important; thus, the second approach (PWM) is considered here. A fundamental requirement for a high frequency switching concept is that the switching frequency of the PWM control must be sufficiently above the natural frequency of the controlled drive system in order to avoid unwanted resonance effects and, furthermore, to obtain an averaged system model for synthesis (see, for instance [28]). Today, the common switching frequencies of PWM operated hydraulic valves are in the range of  $f_{\text{PWM}} \approx 50$  to 100 Hz (see, for instance, [29]). Unfortunately, the natural frequencies of common hydraulic cylinder drives are in the same range as the achievable switching frequencies. One possibility to fulfill the requirement for a high frequency digital valve actuation is to apply a gas loaded hydraulic accumulator in order to lower the natural frequency of the drive system. In recent publications like, for instance in [7], a flatness based control was designed in order to compensate the resulting nonlinearities and the softness due to the

gas loaded accumulator. Compared to other nonlinear controllers one major advantage of the flatness based control is that even the trajectory of the drive system is stabilized. On the other hand, in the flatness approach the desired trajectory and a number of its derivatives with respect to time are necessary, which requires a rather high implementation effort. Furthermore, experiments showed a limited robustness of the closed loop behavior on parameter variations, stick-slip effects and measurement noise. For those reasons in this paper a passivity based control is intended, which in fact does only stabilize the desired equilibrium, but is much easier in its implementation. Moreover, since it is an energy based concept an improved robustness is expected.

The main contribution of this paper is i) the Port Hamiltonian formulation of a hydraulic drive system comprising a hydraulic accumulator suitable for PWM control purposes and ii) the derivation and the simulation based verification of a nonlinear passivity based controller. Furthermore, a discussion of the results, concluding remarks and an outlook to future work are provided at the end of the contribution.

## 2 Formulation of the Problem and Preliminaries

As an example from steel industry in [30] the so called interconnection and damping assignment passivity based control (IDA-PBC) of a single acting ram (SAR) according to Fig. 2 is presented. Its dynamic model is

$$\begin{aligned} \begin{bmatrix} \dot{x} \\ \dot{v} \\ \dot{p} \end{bmatrix} &= \begin{bmatrix} v \\ \frac{1}{m} ((\bar{p} + p) A_1 - d_v v - p_S A_2 - F) \\ \frac{E_{\text{oil}}}{V_0^C + A_1 x} (-A_1 v + Q) \end{bmatrix} \\ &= \underset{\bar{p}=p_S \frac{A_2}{A_1}}{\uparrow} \begin{bmatrix} v \\ \frac{1}{m} (p A_1 - d_v v - F) \\ \frac{E_{\text{oil}}}{V_0^C + A_1 x} (-A_1 v + Q) \end{bmatrix} \end{aligned} \quad (1)$$

with the state variables<sup>1</sup>  $x$  for the position,  $v$  for the velocity and  $p$  for the pressure the input flow rate  $Q$ . The resulting control law for the flow rate into the cylinder reads

$$\begin{aligned} Q &= \alpha (A_1 x + V_0^C) \left( \ln \left( \frac{A_1 x^* + V_0^C}{A_1 x + V_0^C} \right) \right. \\ &\quad \left. + \frac{1}{E_{\text{oil}}} (p^* - p) \right), \end{aligned} \quad (2)$$

which is mainly determined by the desired mass of the compressible fluid in the piston sided chamber

<sup>1</sup> Instead of canonical coordinates in this paper the system state is considered in sensor coordinates, which may result in a better readability for hydraulic engineers.

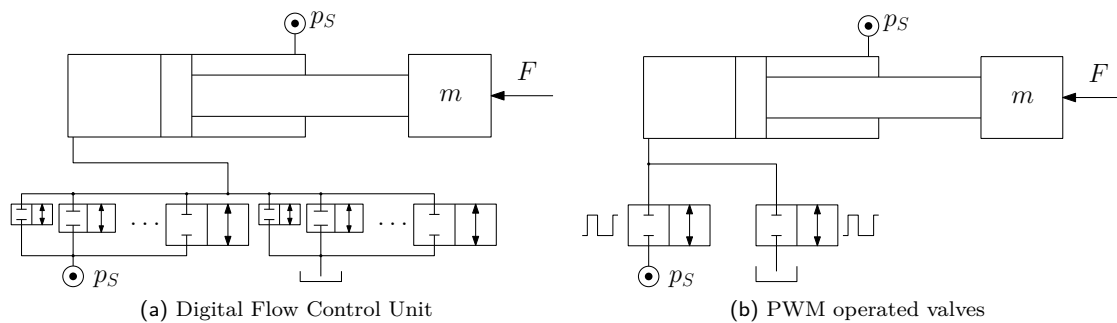


Fig. 1: Digital Hydraulic Concepts

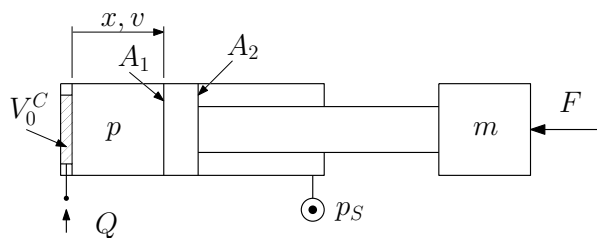


Fig. 2: Hydraulic single acting ram (SAR)

according to material law of the fluid  $\rho = \rho_0 e^{\frac{p-p_0}{E_{oil}}}$  in the desired position  $x^*$  at the load pressure  $p^* = \frac{F}{A_1}$ . The control from Eq. (2) accounts for the nonlinear system behavior due to the pressure build up in the piston chamber and stabilizes the desired equilibrium  $\mathbf{x}_d = [x^* \ 0 \ p^*]^T$ . Furthermore, one major advantage of this controller is that no measurement of the velocity is required. Of course, a pressure measurement is needed in order to estimate the actual load force, which can be done with a dynamic load observer like, for instance, presented in [31].

In this example from the literature the flow rate  $Q$  is realized by a servovalve. As mentioned in the introduction in this paper a PWM valve actuation is intended, which requires a sufficient gap between the switching frequency of the valves and the natural frequency of the drive system. For this purpose the natural frequencies of the considered drive systems are assessed in the following.

After linearization of system (1) and using an exemplary parameter set of a common hydraulic actuator according to Tab. 1 the natural frequency of the linear drive according to Fig. 2 calculates to

$$\omega_{SAR} = \sqrt{\frac{E_{oil} A_1^2}{(V_0^C + A_1 x) m}} \Big|_{x=0.01 \text{ m}} \approx 2\pi \cdot 100 \text{ Hz.} \quad (3)$$

Thus, in this and in many other cases the natural frequency (3) is close to, or even, beyond the feasible switching frequencies mentioned above, which would result in a strong excitation of the drive and

Parameter	Value
dead volume	$V_0^C = 0.05e^{-3} \text{ m}^3$
accumulator volume	$V_0 = 0.32e^{-3} \text{ m}^3$
gas pre-load pressure	$p_0 = 50 \text{ bar}$
polytropic exponent	$\kappa = 1.3$
dead load	$m = 500 \text{ kg}$
cross-section area piston	$A_1 = \frac{0.063^2 \pi}{4} \text{ m}^2$
annulus cross-section area	$A_2 = \frac{(0.063^2 - 0.045^2) \pi}{4} \text{ m}^2$
supply pressure	$p_s = 200 \text{ bar}$
compressibility modulus	$E_{oil} = 16000 \text{ bar}$
viscous friction	$d_v = 1000 \frac{\text{Ns}}{\text{m}}$

Tab. 1: Exemplary parameters of a common linear hydraulic drive

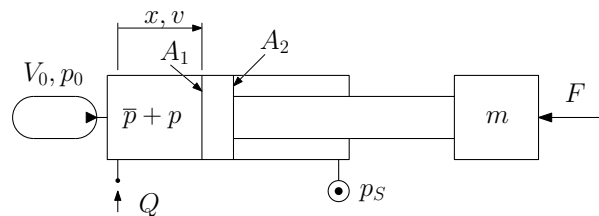


Fig. 3: Single acting ram using a gas loaded accumulator for pressure attenuation (SAR)

would lead to large fluctuations in pressure and velocity due to the switching of the digital valves. In order to prevent a scattering movement of the drive the switching frequency must be sufficiently above the natural frequency of the drive. Since the switching frequency is limited by the available switching valves, the natural frequency of the drive must be lowered, which can be achieved by the application of a gas loaded accumulator according to Fig. 3. In the accumulator the elasticity of the gas spring of the accumulator is much softer than the oil stiffness. Thus, for simplicity and with regard to [32], the compressibility of the fluid is completely neglected and the dynamic model of the drive configuration

reads

$$\begin{aligned} \begin{bmatrix} \dot{x} \\ \dot{v} \\ \dot{p} \end{bmatrix} &= \begin{bmatrix} \frac{1}{m} ((\bar{p} + p) A_1 - d_v v - p_S A_2 - F) \\ \frac{\varkappa(\bar{p} + p)}{V_0 \left(\frac{p_0}{\bar{p} + p}\right)^{\frac{1}{\varkappa}}} (-A_1 v + Q) \\ v \end{bmatrix} \\ &\stackrel{\bar{p} = p_S \frac{A_2}{A_1}}{=} \begin{bmatrix} \frac{1}{m} (p A_1 - d_v v - F) \\ \frac{\varkappa(\bar{p} + p)}{V_0 \left(\frac{p_0}{\bar{p} + p}\right)^{\frac{1}{\varkappa}}} (-A_1 v + Q) \\ v \end{bmatrix} \end{aligned} \quad (4)$$

with the same state vector  $\mathbf{x} = [x \ v \ p]^T$  as of system (1). Again, after linearization of system (4) and with the exemplary parameter set from Tab. 1 the natural frequency of the  $\widehat{\text{SAR}}$  can be assessed by

$$\begin{aligned} \omega_{\widehat{\text{SAR}}} &= \sqrt{\frac{\varkappa(\bar{p} + p) A_1^2}{V_0 m} \left(\frac{p_0}{\bar{p} + p}\right)^{-\frac{1}{\varkappa}}} \\ &\approx 2\pi \cdot 8 \text{ Hz} \ll 2\pi \cdot f_S, \end{aligned} \quad (5)$$

which is sufficiently below the feasible switching frequency for a smooth movement of the drive. However, the application of the gas loaded accumulator results in a probably unwanted softness of the drive, which must be compensated by the control. Linear hydraulic drives according to Fig. 3 were investigated experimentally already in [33] or even with an energetically high efficient switching converter concept employing a flatness based control in [34]. In the following the passivity based modeling and control of a digital hydraulic drive according to Fig. 3 is presented.

### 3 Port Hamiltonian Representation of the Drive System

For the design of a passivity based control a transformation of the model according to Eq. (4) to the form of a Port Hamiltonian System is advantageous. For this purpose the energy stored in the system must be calculated, which is shown in the following.

A basic property of system (4) is that the fluid is assumed to be incompressible and the pressure build up takes place with regard to the gas spring of the accumulator, which dominates the elasticity of the hydro-mechanical spring mass oscillator interacting with the dead load. With regard to Fig. 4 the gas spring in the accumulator behaves according to a polytropic change of state

$$p_0 V_0^\varkappa = (\bar{p} + p) V_G^\varkappa = \text{const.} \quad (6)$$

with the housing volume of the accumulator  $V_0$ , the gas pre-load pressure  $p_0$  and the polytropic exponent  $\varkappa$ . With the gas volume  $V_G$  from Eq. (6) in

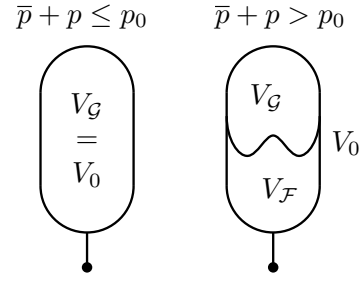


Fig. 4: Gas-loaded accumulator; left: empty; right: fluid, respectively, energy is stored

the operating point  $\bar{p} + p$  the corresponding fluid volume in the accumulator reads

$$V_F = V_0 - V_G = V_0 \left(1 - \left(\frac{p_0}{\bar{p} + p}\right)^{\frac{1}{\varkappa}}\right). \quad (7)$$

Below the gas pre-load pressure  $p_0$  no fluid and, thus, no energy is stored in the accumulator; to avoid this unwanted state the operating pressure must fulfill  $\bar{p} + p \geq p_0$ . Then the energy stored in the gas spring of the accumulator calculates to

$$\begin{aligned} E_G &= - \int_{V_1}^{V_2} p dV_G = - \int_{-\bar{p} + p_0}^p p \frac{\partial V_G}{\partial p} dp \\ &= \frac{V_0}{\varkappa - 1} \left( \left(\frac{p_0}{\bar{p} + p}\right)^{\frac{1}{\varkappa}} (\bar{p} + p) - p_0 \right). \end{aligned} \quad (8)$$

Under the assumption that the compressibility of the oil is completely neglected, the energy of the incompressible part of the fluid according to the displacement with regard to the operating point  $\bar{p} = p_S \frac{A_2}{A_1}$  follows to

$$\begin{aligned} E_F &= - \int_{V_1}^{V_2} \bar{p} dV_F = -\bar{p} \int_{-\bar{p} + p_0}^p \frac{\partial V_F}{\partial p} dp \\ &= -\bar{p} V_0 \left(1 - \left(\frac{p_0}{\bar{p} + p}\right)^{\frac{1}{\varkappa}}\right). \end{aligned} \quad (9)$$

As a consequence, the sum  $E_G + E_F$  has a (local) minimum at the equilibrium with  $p = 0$  in case of  $F = 0$ . With the kinetic energy  $T = \frac{1}{2} m v^2$  the Hamiltonian respectively the total energy stored in the system reads

$$H(\mathbf{x}) = E_G + E_F + \frac{1}{2} m v^2. \quad (10)$$

The dynamic system from Eq. (4) can be written in the form of a Port Hamiltonian System (PH-system)

$$\dot{\mathbf{x}} = (\mathbf{J}(\mathbf{x}) - \mathbf{R}(\mathbf{x})) \left( \frac{\partial H}{\partial \mathbf{x}} \right)^T + \mathbf{g}_u(\mathbf{x}) Q + \mathbf{g}_d F \quad (11)$$

with

$$\mathbf{J}(\mathbf{x}) = \begin{bmatrix} 0 & \frac{1}{m} & 0 \\ -\frac{1}{m} & 0 & \zeta \\ 0 & -\zeta & 0 \end{bmatrix},$$

$$\mathbf{R}(\mathbf{x}) = \begin{bmatrix} 0 & 0 & 0 \\ 0 & \frac{d_v}{m} & 0 \\ 0 & 0 & 0 \end{bmatrix},$$

$$\mathbf{g}_u(\mathbf{x}) = \begin{bmatrix} 0 \\ 0 \\ \frac{m}{A_1} \zeta \end{bmatrix}, \quad \mathbf{g}_d = \begin{bmatrix} 0 \\ -\frac{1}{m} \\ 0 \end{bmatrix},$$

$$\zeta = \frac{A_1 \varkappa (\bar{p} + p)}{V_0 m} \left( \frac{p_0}{\bar{p} + p} \right)^{-\frac{1}{\varkappa}} > 0$$

and the output

$$y = \mathbf{g}_u^T \left( \frac{\partial H}{\partial \mathbf{x}} \right)^T = p.$$

In a PH-system the skew symmetric matrix  $\mathbf{J}(\mathbf{x})$  describes the flow of energy within the system;  $\mathbf{R}(\mathbf{x})$  is positive (semi-) definite and represents the dissipating elements of the system. This insight into the physics of the system dynamics is helpful for the design of a controller as presented in the following section.

## 4 Passivity Based Control

Due to the fact that the system from Fig. 3 represents a PH-system according to Eq. (11) a passivity based controller can be designed, which is closely related to Lyapunov's theory. This means that the controller design requires a certain storage function in form of the Hamiltonian  $H_d$  in order to guarantee stability and, furthermore, to achieve the desired performance of the closed loop system.

### 4.1 Coordinate Transformation

In order to simplify the search for a qualified Hamiltonian  $H_d$  for the closed loop system a transformation into new coordinates is helpful. For this purpose the following set of partial differential equations

$$\frac{\partial C(\mathbf{x})}{\partial \mathbf{x}} (\mathbf{J}(\mathbf{x}) - \mathbf{R}(\mathbf{x})) = \mathbf{0} \quad (12)$$

represents the restrictions for a so called Casimir function  $C(\mathbf{x})$ , which is a structural invariant of the system (see, for instance, [35]). The resulting

partial differential equations

$$\begin{aligned} -\frac{1}{m} \frac{\partial C}{\partial v} &= 0 \\ \frac{1}{m} \frac{\partial C}{\partial x} - \frac{d_v}{m^2} \frac{\partial C}{\partial v} - \frac{A_1 \varkappa (\bar{p} + p)}{m V_0 \left( \frac{p_0}{\bar{p} + p} \right)^{\frac{1}{\varkappa}}} \frac{\partial C}{\partial p} &= 0 \\ \frac{A_1 \varkappa (\bar{p} + p)}{m V_0 \left( \frac{p_0}{\bar{p} + p} \right)^{\frac{1}{\varkappa}}} \frac{\partial C}{\partial v} &= 0 \end{aligned} \quad (13)$$

are solved by

$$C(\mathbf{x}) = A_1 x + V_0 \underbrace{\left( 1 - \left( \frac{p_0}{\bar{p} + p} \right)^{\frac{1}{\varkappa}} \right)}_{V_{\mathcal{F}}} = z, \quad (14)$$

which allows a convenient physical interpretation:  $C(\mathbf{x}) = A_1 x + V_{\mathcal{F}}$  represents the total amount of fluid in the system (4) comprising the cylinder chamber and the gas loaded accumulator, which remains constant as long as no energy passes the input port  $Q$ , in other words, all valves are closed. Using  $C(\mathbf{x}) = z$  as a coordinate transformation for the sub-state  $p$  the resulting system reads

$$\begin{aligned} \dot{\mathbf{z}} &= \left( \tilde{\mathbf{J}}(\mathbf{z}) - \tilde{\mathbf{R}}(\mathbf{z}) \right) \left( \frac{\partial \tilde{H}}{\partial \mathbf{z}} \right)^T + \tilde{\mathbf{g}}_u(\mathbf{z}) Q + \mathbf{g}_d F \\ &= \tilde{\mathbf{f}}(\mathbf{z}, F) + \tilde{\mathbf{g}}_u(\mathbf{z}) Q \end{aligned} \quad (15)$$

with

$$\tilde{\mathbf{J}}(\mathbf{z}) = \begin{bmatrix} 0 & \frac{1}{m} & 0 \\ -\frac{1}{m} & 0 & 0 \\ 0 & 0 & 0 \end{bmatrix}$$

$$\tilde{\mathbf{R}}(\mathbf{z}) = \begin{bmatrix} 0 & 0 & 0 \\ 0 & \frac{d_v}{m} & 0 \\ 0 & 0 & 0 \end{bmatrix}, \quad \tilde{\mathbf{g}}_u(\mathbf{z}) = \begin{bmatrix} 0 \\ 0 \\ 1 \end{bmatrix}$$

now in the new coordinates  $\mathbf{z} = [x \ v \ z]^T$ .

### 4.2 Interconnection and Damping Assignment

The main intention of the Interconnection and Damping Assignment (IDA) concept is to find a Hamiltonian  $\tilde{H}_d$  and to design the matrices  $\tilde{\mathbf{J}}_d(\mathbf{z})$  and  $\tilde{\mathbf{R}}_d(\mathbf{z})$  such that the closed loop system is stable and provides the desired performance. One possibility is an extension of the original Hamiltonian by an augmented one as

$$\tilde{H}_d = \tilde{H} + \tilde{H}_a, \quad (16)$$

which means that the energy of the original system is again part of the closed loop system. Furthermore, the choice

$$\tilde{\mathbf{J}}_d(\mathbf{z}) = \tilde{\mathbf{J}}(\mathbf{z}), \quad \tilde{\mathbf{R}}_d(\mathbf{z}) = \begin{bmatrix} 0 & 0 & 0 \\ 0 & \frac{d_v}{m} & 0 \\ 0 & 0 & \frac{\alpha}{\beta} \end{bmatrix}, \quad (17)$$

results in the same structural energy flow in the system and, moreover, an additional damping coefficient  $\frac{\alpha}{\beta}$  in  $\tilde{\mathbf{R}}_d(\mathbf{z})$ . For the calculation of the augmented Hamiltonian  $\tilde{H}_a$  the so called PBC matching equation

$$\mathbf{G}_u^\perp(\mathbf{z})\tilde{\mathbf{f}}(\mathbf{z}, F) = \mathbf{G}_u^\perp(\mathbf{z})\left(\tilde{\mathbf{J}}_d(\mathbf{z}) - \tilde{\mathbf{R}}_d(\mathbf{z})\right)\left(\frac{\partial\tilde{H}}{\partial\mathbf{z}} + \frac{\partial\tilde{H}_a}{\partial\mathbf{z}}\right)^T \quad (18)$$

with the left annihilator

$$\mathbf{G}_u^\perp(\mathbf{z}) = \begin{bmatrix} 1 & 0 & 0 \\ 0 & 1 & 0 \end{bmatrix} \quad (19)$$

must be fulfilled. Equation (18) is a set of partial differential equations in  $\tilde{H}_a(x, v, z)$ , which reads

$$\frac{1}{m}\left(F - \frac{d_v}{m}\frac{\partial\tilde{H}_a(x, v, z)}{\partial v} - \frac{\partial\tilde{H}_a(x, v, z)}{\partial x}\right) = 0$$

$$\frac{1}{m}\frac{\partial\tilde{H}_a(x, v, z)}{\partial v} = 0$$

and which is solved by the augmented Hamiltonian  $\tilde{H}_a(\mathbf{z}) = Fx + f_a(z)$ , where  $f_a$  is an arbitrary function in  $z$ . The desired Hamiltonian is chosen to

$$\tilde{H}_d(\mathbf{z}) = \tilde{H} + \tilde{H}_a = \tilde{H} + Fx + \underbrace{\frac{1}{2}\beta(z^* - z)^2}_{E_\mathcal{E}} - p^*z, \quad (20)$$

where the original energy of the system is augmented by the weighted energy  $E_\mathcal{E}$  of the control error between the actual and the desired fluid volume in the system. Furthermore, in  $\tilde{H}_d$  the work of the load force  $F$  according to its displacement is compensated by its hydraulic pendant  $p^*z$ , the last term in Eq. (20) under the assumptions  $F = p^*A_1$  and  $z > 0$ . In order to proof stability of the closed loop system  $\tilde{H}_d$  will be investigated around the equilibrium  $\mathbf{z} = \mathbf{z}_d$ . There the desired Hamiltonian  $\tilde{H}_d$  fulfills the following conditions

$$\tilde{H}_d(\mathbf{z}) > \tilde{H}_d(\mathbf{z}_d) \quad \forall \mathbf{z} \neq \mathbf{z}_d \quad (21)$$

$$\left(\frac{\partial\tilde{H}_d}{\partial\mathbf{z}}\right)^T \Big|_{\mathbf{z}=\mathbf{z}_d} = \begin{bmatrix} F - p^*A_1 \\ 0 \\ 0 \end{bmatrix} \underset{F=p^*A_1}{=} \mathbf{0} \quad (22)$$

$$\left(\frac{\partial^2\tilde{H}_d}{\partial\mathbf{z}^2}\right) \Big|_{\mathbf{z}=\mathbf{z}_d} = m\zeta \begin{bmatrix} A_1 & 0 & -1 \\ 0 & \frac{1}{\zeta} & 0 \\ -1 & 0 & \frac{\beta}{m\zeta} + \frac{1}{A_1} \end{bmatrix} \underset{p=p^*}{>} \mathbf{0}, \quad (23)$$

which means that  $\tilde{H}_d$  has a local minimum at the desired equilibrium  $\mathbf{z}_d$ . Thus, the desired Hamiltonian  $\tilde{H}_d$  is a qualified candidate for a

Lyapunov function and, thus, the desired equilibrium  $\mathbf{z}_d = [x^* \ 0 \ z^*]^T$  or, respectively,  $\mathbf{x}_d = [x^* \ 0 \ p^*]^T$  can be stabilized with the control law

$$Q = (\tilde{\mathbf{g}}_u^T(\mathbf{z})\tilde{\mathbf{g}}_u(\mathbf{z}))^{-1}\tilde{\mathbf{g}}_u^T(\mathbf{z})\left\{\tilde{\mathbf{J}}_d(\mathbf{z})\left(\frac{\partial\tilde{H}_d}{\partial\mathbf{z}}\right)^T - \tilde{\mathbf{R}}_d(\mathbf{z})\left(\frac{\partial\tilde{H}_d}{\partial\mathbf{z}}\right)^T - \tilde{\mathbf{f}}(\mathbf{z}, F)\right\}$$

$$= \alpha(z^* - z) + \frac{\alpha}{\beta}\left[\left(\frac{V_0}{A_1x^* + V_0 - z^*}\right)^\alpha - \left(\frac{V_0}{A_1x + V_0 - z}\right)^\alpha\right]$$

$$= \alpha\left[A_1(x^* - x) + V_0\left(\left(\frac{p_0}{\bar{p} + p}\right)^{\frac{1}{\alpha}} - \left(\frac{p_0}{\bar{p} + p^*}\right)^{\frac{1}{\alpha}}\right)\right] + \underbrace{\frac{\alpha}{\beta}(p^* - p)}_{\text{damping injection}}. \quad (24)$$

The last term in Eq. (24) represents an injection of damping into the closed loop system. This can be shown by using the Hamiltonian from Eq. (20) without the energy of the control error  $E_\mathcal{E}$ , which reads

$$\tilde{H}_{DI} = \tilde{H}_d - E_\mathcal{E} = \tilde{H} + Fx - p^*z. \quad (25)$$

Then the output (in original coordinates)

$$y = \mathbf{g}_u^T(\mathbf{x})\left(\frac{\partial H_{DI}}{\partial\mathbf{x}}\right)^T = p - p^*, \quad (26)$$

is called collocated to the input  $Q$ . In this context, a simple feedback of the collocated output with the amplification  $\frac{\alpha}{\beta}$  according to  $\mathbf{R}_d(\mathbf{x})$  from Eq. (17) is

$$Q_{DI} = -\frac{\alpha}{\beta}y = -\frac{\alpha}{\beta}\mathbf{g}_u^T(\mathbf{x})\left(\frac{\partial H_{DI}}{\partial\mathbf{x}}\right)^T = \frac{\alpha}{\beta}(p^* - p) \quad (27)$$

and leads to

$$\frac{d}{dt}H_{DI} = -\left(\frac{\partial H_{DI}}{\partial\mathbf{x}}\right)\left(\mathbf{R}(\mathbf{x}) + \mathbf{g}_u(\mathbf{x})\left[\frac{\alpha}{\beta}\mathbf{g}_u^T(\mathbf{x})\right]\left(\frac{\partial H_{DI}}{\partial\mathbf{x}}\right)^T\right) = -d_v v^2 - \frac{\alpha}{\beta}(p^* - p)^2 \leq 0, \quad (28)$$

which means that energy is dissipated from the closed loop system as long as pressure fluctuations  $p$  with regard to the desired equilibrium load pressure  $p^*$  occur. For  $\beta \rightarrow \infty$  only natural damping

$d_v$  is present, respectively, no additional damping is injected to the system and, thus, only the fluid volume necessary for the desired equilibrium is controlled by Eq. (24).

## 5 Load Observer

The controller from Eq. (24) requires the knowledge of the desired load pressure  $p^*$  according to the load force  $F$ . Furthermore, it is assumed, that the actual pressure  $p$  and the piston position  $x$  are measured. The desired load pressure, respectively the load force can be calculated by a reduced observer like presented, for instance, in [36, 37]. Thus, the observer design is sketched just for completeness, respectively, in order to give the reader the possibility to reproduce the results. In the following a constant load force, i.e.  $\dot{F} = 0$  is assumed. Then the dynamic system of the unknown states reads

$$\begin{bmatrix} \dot{v} \\ \dot{F} \end{bmatrix} = \begin{bmatrix} -\frac{d_v}{m} & -\frac{1}{m} \\ 0 & 0 \end{bmatrix} \begin{bmatrix} v \\ F \end{bmatrix} + \begin{bmatrix} \frac{1}{m} ((\bar{p} + p) A_1 - p_S A_2) \\ 0 \end{bmatrix}. \quad (29)$$

With the transformation

$$\begin{aligned} w_1 &= v + k_1 x \\ w_2 &= F + k_2 x \end{aligned} \quad (30)$$

the system from Eq. (29) follows to

$$\begin{bmatrix} \dot{w}_1 \\ \dot{w}_2 \end{bmatrix} = \underbrace{\begin{bmatrix} k_1 - \frac{d_v}{m} & -\frac{1}{m} \\ k_2 & 0 \end{bmatrix}}_{\mathbf{A}_O} \begin{bmatrix} w_1 \\ w_2 \end{bmatrix} + \begin{bmatrix} -k_1^2 + \frac{d_v}{m} k_1 + \frac{k_2}{m} & \frac{A_1}{m} \\ -k_1 k_2 & 0 \end{bmatrix} \begin{bmatrix} x \\ p \end{bmatrix} \quad (31)$$

with the observer parameters  $k_i$ ,  $i = 1, 2$ . With the estimation error

$$\mathbf{e} = \begin{bmatrix} v - \hat{v} \\ F - \hat{F} \end{bmatrix} = \begin{bmatrix} w_1 - \hat{w}_1 \\ w_2 - \hat{w}_2 \end{bmatrix} \quad (32)$$

the dynamics of the observer calculates to

$$\dot{\mathbf{e}} = \mathbf{A}_O \mathbf{e}. \quad (33)$$

Since  $\mathbf{A}_O$  is time invariant it is sufficient that the real parts of its eigenvalues are negative in order to obtain stability of the error dynamics. This can be achieved with a proper choice of the parameters  $k_i$ , and then the observed load force and, thus, the desired pressure follows to

$$p^* = \frac{\hat{F}}{A_1} = \frac{w_2 - k_2 x}{A_1}. \quad (34)$$

## 6 Simulations and Discussion

In Fig. 5 the block diagram of the Interconnection and Damping Assignment Passivity Based Control (IDA-PBC) is illustrated. Due to the fact that the switching frequency of the digital valves is much higher than the natural frequency of the drive the flow rate  $Q$  with respect to the PWM duty ratio  $\kappa$  can be modeled as

$$Q = \begin{cases} \kappa Q_N \sqrt{\frac{p_S - (\bar{p} + p)}{p_N}} & 0 < \kappa \leq 1 \\ 0 & \kappa = 0 \\ \kappa Q_N \sqrt{\frac{(\bar{p} + p) - p_T}{p_N}} & -1 \leq \kappa < 0 \end{cases}, \quad (35)$$

which incorporates the square root characteristic of the digital valves<sup>2</sup>. Thus, the flow rate  $Q$  is proportional to the duty ratio  $\kappa$  at the load pressure  $\bar{p} + p$ . Since the control law from Eq. (24) calculates an input flow rate a so called *valve compensation* is necessary, which calculates in accordance with Eq. (35) to

$$\kappa = \begin{cases} \frac{Q}{Q_N} \sqrt{\frac{p_N}{p_S - (\bar{p} + p)}} \leq 1 & Q > 0 \\ 0 & Q = 0 \\ \frac{Q}{Q_N} \sqrt{\frac{p_N}{(\bar{p} + p) - p_T}} \geq -1 & Q < 0 \end{cases} \quad (36)$$

under the assumptions  $p_T < \bar{p} + p < p_S$  and  $-1 \leq \kappa \leq 1$ .

The simulations were carried out in *Matlab/Simulink* according to the block scheme from Fig. 5 using a variable step solver ode45 (Dormand-Prince). The valves used in the simulations have a nominal flow rate of  $Q_N = 40 \text{ l/min}$  at a pressure drop of  $p_N = 5 \text{ bar}$ . For the PWM switching of the valves a frequency of  $f_{\text{PWM}} = 50 \text{ Hz}$  was used. For a sufficient smooth quantization of the duty ratio  $\kappa$  the sampling frequency of the PWM signal was chosen to  $f_S = 10 \text{ kHz}$ , which results in a PWM resolution of  $\Delta\kappa = \frac{f_{\text{PWM}}}{f_S} = 0.5\%$  with regard to the periodic time  $T_{\text{PWM}} = \frac{1}{f_{\text{PWM}}} = 20 \text{ ms}$ . It is worth mentioning that the computational effort for the passivity based control is rather low compared to other nonlinear control methods due to the simplicity of the control law from Eq. (24). The controller parameters  $\alpha$  and  $\beta$  were chosen empirically, however, it is expected that on a real test axis the controller parameters must be optimized due to some additional effects, like unknown friction or other parasitic effects, which were not considered in the modelling.

In Fig. 6 simulation results for a ramp-like movement at a piston velocity of  $v_d = 250 \frac{\text{mm}}{\text{s}}$  are depicted. In the upper diagrams the desired and the

<sup>2</sup> For simplicity reasons the violation of the Lipschitz condition due to the square root function is neglected here, since critical operating points are not considered in this paper.

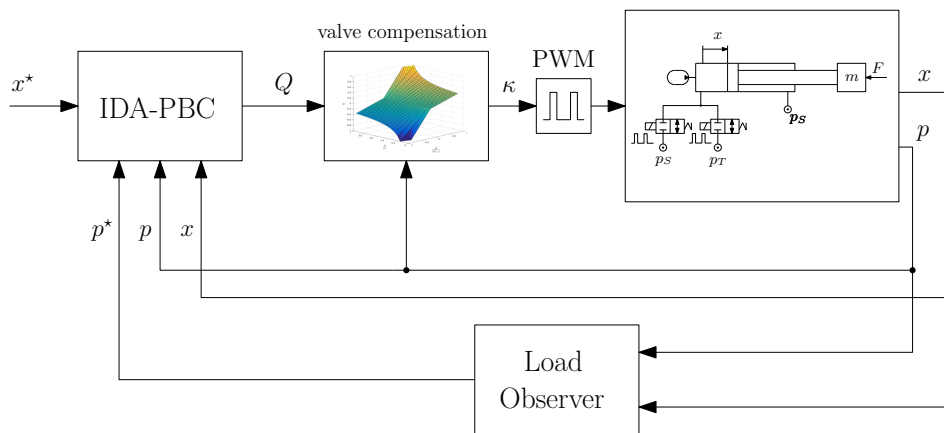


Fig. 5: Block Scheme of the Interconnection and Damping Assignment Passivity Based Control (IDA-PBC)

actual position of the piston are opposed. The simulations show a smooth movement of the piston at a switching frequency of the PWM control of  $f_{\text{PWM}} = 50 \text{ Hz}$  due to the pressure attenuation effect of the gas loaded accumulator. At the simulation time  $t = 2 \text{ s}$  a load force of  $F = 10 \text{ kN}$  is applied to the piston rod with a rate of  $50 \text{ kN/s}$ . With the load observer the deviation due to the process force can be completely compensated. In the middle diagram of Fig. 6a the actual pressure  $\bar{p} + p$  and the desired pressure  $\bar{p} + p^*$  according to the load observer are illustrated. During the movement of the piston some pressure fluctuations occur due to the switching of the digital hydraulic valves. The magnitude of the pressure pulsations can be reduced by a larger gas-loaded accumulator, which in turn slows down the natural dynamics of the drive system. Thus, the system design is always a compromise between pressure ripples and response dynamics. In the presented case the pressure ripples are acceptable with respect to the desired control performance. The lower diagram in the same figure shows the actual mean flow rate  $\bar{Q}_{IN}$  according to Eq. (24), which is averaged over one switching period  $T_{\text{PWM}} = \frac{1}{f_{\text{PWM}}}$ . In the lower diagram the actual valve switching and the duty ratio  $\kappa$  according to Eq. (36) are presented. The hydraulic switching valves were considered as seat type valves with a switching time of  $t_S = 2 \text{ ms}$  for full opening. Due to their response dynamics and the small control error in the desired rest positions the digital valves are not fully switched anymore, i.e. they act in a so called ballistic mode (see, for instance, [38]). Shrinking a dead band around the desired rest position an arbitrary accuracy can be achieved, at least theoretically. In practice the achievable accuracy is mainly influenced by the design of the valves and their dynamic switching, the load pressure and the sample time of the signal pro-

cessing unit. In Fig. 7a the states  $\hat{v}$  and  $\hat{F}$  of the observer are opposed to their actual values. The observer parameters were chosen quite soft in order to show the difference between the actual and the observed states. The closed loop behavior can be improved significantly by a better tuning of the observer and controller parameters, respectively. In Fig. 7b the effect of the damping injection is illustrated. The diagrams show that the oscillations due to the low natural damping ( $\beta \rightarrow \infty$ ) in combination with the softness resulting from the gas loaded accumulator can be reduced significantly by the injection of additional damping according to Eq. (27).

## 7 Conclusion and Outlook

In this paper an IDA-PBC for a digitally actuated linear hydraulic drive was presented. With the application of a gas loaded accumulator to the piston chamber of a single acting hydraulic ram the natural frequency can be tuned sufficiently below the today feasible hydraulic switching frequencies for a proper PWM actuation of the drive. The use of cheap and robust digital hydraulic valves allows a low cost implementation of the overall hydraulic drive system, which results in lower installation costs and, furthermore, in lower energy consumption compared to drives controlled by piloted servovalves. With the use of high response digital valves corresponding large flow rates can be achieved within a few milliseconds. Since the digital valves also have a large nominal flow rate high drive velocities can be realized. In fact, the gas loaded accumulator makes the system soft, which on the other hand could be advantageous for applications where force control is intended. Furthermore, since additional damping can be injected to the drive system with the presented controller also, for instance, active sus-



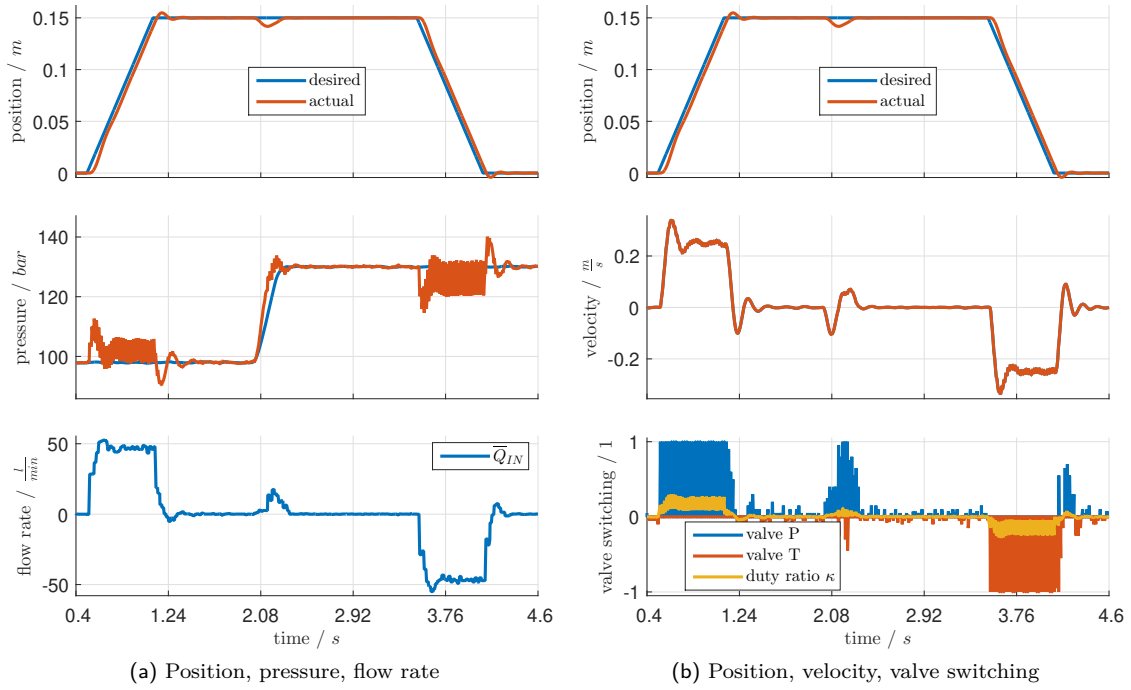


Fig. 6: Simulation results

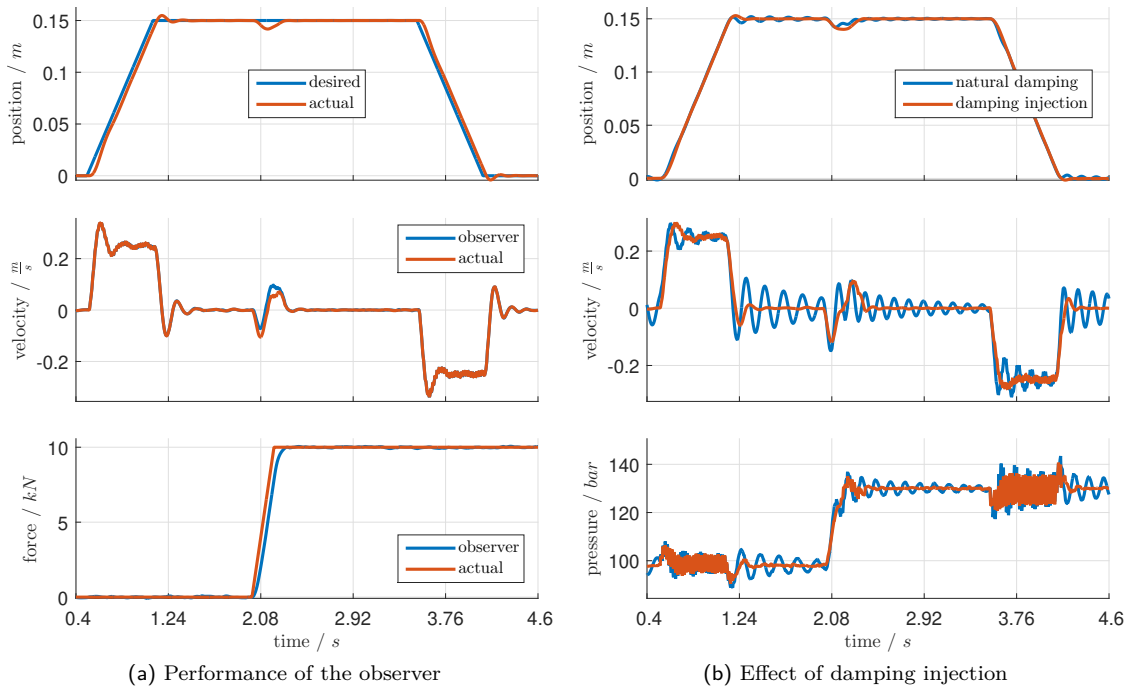


Fig. 7: Simulation results

pensions for vehicles can be realized with the advantages of digital hydraulics. The nonlinear energy based controller achieves satisfying results in the presented simulations. Future work will be devoted to experimental investigations of the presented controller. Furthermore, in some applications a pipeline between the cylinder and the accumulator is desirable for maintenance reasons. Thus, also the influence of the pipe line dynamics on the system design will be a part of future investigations.

## Acknowledgment

This work has been supported by the COMET-K2 Center of the Linz Center of Mechatronics (LCM) funded by the Austrian federal government and the federal state of Upper Austria.

## References

- [1] Alberto Isidori. *Nonlinear Control Systems*. Springer London, 1995.
- [2] Michel Fliess, Jean Lévine, Phillipe Martin, and Pierre Rouchon. Flatness and Defect of Nonlinear Systems: Introductory Theory and Examples. *International Journal of Control*, 61(6):1327–1361, jun 1995.
- [3] Michel Fliess and Joachim Rudolph. Local "tracking observers" for flat systems. In *Proceedings of the Symposium on Control, Optimization and Supervision, CESA '96 IMACS Multiconference, Lille, France*, pages 213–217, 1996.
- [4] Andreas Kugi, Kurt Schlacher, and Rainer Novak. Nonlinear Control in Rolling Mills: A New Perspective. *IEEE Transactions on Industry Applications*, 37(5):1394–1402, 2001.
- [5] Florian Kock and Cornelius Ferrari. Flatness-Based High Frequency Control of a Hydraulic Actuator. *Journal of Dynamic Systems, Measurement, and Control*, 134(2):021003, 2012.
- [6] Rainer Haas, Christoph Hinterbichler, Evgeny Lukachev, and Markus Schöberl. Optimal Digital Hydraulic Feed-Forward Control applied to Simple Cylinder Drives. In *Proceedings of the 8<sup>th</sup> Workshop on Digital Fluid Power, May 24–25, Tampere, Finland*, 2016.
- [7] Helmut Kogler and Rudolf Scheidl. Linear Motion Control with a Low Power Hydraulic Switching Converter - Part II: Flatness Based Control. *Proceedings of the Institution of Mechanical Engineers, Part I: Journal of Systems and Control Engineering*, 229(9):818–828, may 2015.
- [8] Giorgio Bartolini, Leonid Fridman, Alessandro Pisano, and Elio Usai. *Modern Sliding Mode Control Theory*. Springer Berlin Heidelberg, 2008.
- [9] Yueying Wang, Hao Shen, Hamid Reza Karimi, and Dengping Duan. Dissipativity-Based Fuzzy Integral Sliding Mode Control of Continuous-Time T-S Fuzzy Systems. *IEEE Transactions on Fuzzy Systems*, 26(3):1164–1176, jun 2018.
- [10] Yueying Wang, Hamid Reza Karimi, Hao Shen, Zhijun Fang, and Mingxin Liu. Fuzzy-Model-Based Sliding Mode Control of Nonlinear Descriptor Systems. *IEEE Transactions on Cybernetics*, pages 1–11, 2018.
- [11] Yueying Wang, Hamid Reza Karimi, Hak-Keung Lam, and Hao Shen. An Improved Result on Exponential Stabilization of Sampled-Data Fuzzy Systems. *IEEE Transactions on Fuzzy Systems*, pages 1–1, 2018.
- [12] Pey-Chung CHEN and Ming-Chang SHIH. An Experimental Study on the Position Control of a Hydraulic Cylinder using a Fuzzy Logic Controller. *JSME international journal. Ser. 3, Vibration, control engineering, engineering for industry*, 34(4):481–489, 1991.
- [13] Q.P. Ha, Q.H. Nguyen, D.C. Rye, and H.F. Durrant-Whyte. Fuzzy Sliding-Mode Controllers with Applications. *IEEE Transactions on Industrial Electronics*, 48(1):38–46, 2001.
- [14] Mete Kalyoncu and Mustafa Haydim. Mathematical Modelling and Fuzzy Logic Based Position Control of an Electrohydraulic Servosystem with Internal Leakage. *Mechatronics*, 19(6):847–858, sep 2009.
- [15] Q.P. Ha, Q.H. Nguyen, D.C. Rye, and H.F. Durrant-Whyte. Impedance Control of a Hydraulically actuated Robotic Excavator. *Automation in Construction*, 9(5-6):421–435, sep 2000.
- [16] Andreas Kugi and Wolfgang Kemmetmüller. Impedance Control of Hydraulic Piston Actuators. *IFAC Proceedings Volumes*, 37(13):961–966, sep 2004.
- [17] Thiago Boaventura, Jonas Buchli, Claudio Semini, and Darwin G. Caldwell. Model-Based Hydraulic Impedance Control for Dynamic Robots. *IEEE Transactions on Robotics*, 31(6):1324–1336, dec 2015.

- [18] Romeo Ortega, Arjan van der Schaft, Bernhard Maschke, and Gerardo Escobar. Interconnection and Damping Assignment Passivity-Based Control of Port-Controlled Hamiltonian Systems. *Automatica, Elsevier Science Ltd.*, 38(4):585–596, apr 2002.
- [19] Romeo Ortega, Arjan van der Schaft, Fernando Castanos, and Alessandro Astolfi. Control by Interconnection and Standard Passivity-Based Control of Port-Hamiltonian Systems. *IEEE Transactions on Automatic Control*, 53(11):2527–2542, dec 2008.
- [20] Rudolf Scheidl, Michael Garstenauer, and Bernhard Manhartgruber. Switching type control of hydraulic drives - A promising perspective for advanced actuation in agricultural machinery. In *SAE Technical Paper Series*. SAE International, sep 2000.
- [21] Bernhard Manhartgruber, Gudrun Mikota, and Rudolf Scheidl. Modelling of a Switching Control Hydraulic System. *Mathematical and Computer Modelling of Dynamical Systems*, 11(3):329–344, sep 2005.
- [22] Matti Linjama and Matti Vilenius. Digital Hydraulics - Towards Perfect Valve Technology. In *Proceedings of The 10<sup>th</sup> Scandinavian International Conference on Fluid Power, SICFP'07, May 21-23, Tampere, Finland*, volume 1(3), pages 181–196, 2007.
- [23] Matti Linjama. Digital Fluid Power - State of the Art. In *12<sup>th</sup> Scandinavian International Conference on Fluid Power, SICFP'11, May 18-20, Tampere, Finland*, volume 3(4), pages 331–353, 2011.
- [24] Bernd Winkler. Development of a fast low-cost switching valve for big flow rates. In *Proceedings of the 3<sup>rd</sup> FPNI PhD Symposium on Fluid Power, Terassa, Spain*, pages 599–606, 2004.
- [25] Andreas Plöckinger and Rudolf Scheidl. Development and laboratory tests of a cheap, robust and fast check valve for industrial applications. In *Proceedings of the 9<sup>th</sup> Scandinavian International Conference on Fluid Power, Linköping, Sweden*, 2005.
- [26] Matti Linjama. Digital Hydraulics Research at IHA. In *Proceedings of The 1<sup>st</sup> Workshop on Digital Fluid Power, 3<sup>rd</sup> October, Tampere, Finland*, 2008.
- [27] Rudolf Scheidl, Bernhard Manhartgruber, and Bernd Winkler. Hydraulic Switching Control - Principles and State of the Art. In *Proceedings of the First Workshop on Digital Fluid Power, DFP08, Tampere, Finland*, 2008.
- [28] Andreas Kugi. *Nonlinear Control based on Physical Models*. Springer, 2001.
- [29] Bernd Winkler. Recent Advances in Digital Hydraulic Components and Applications. In *Proceedings of the 9<sup>th</sup> Workshop on Digital Fluid Power (DFP17)*, 2017.
- [30] Gernot Grabmair, Kurt Schlacher, and Andreas Kugi. Geometric Energy-Based Analysis and Controller Design of Hydraulic Actuators applied in Rolling Mills. In *ECC03 CD publication, Cambridge, Great Britain*, 2003.
- [31] Gernot Grabmair and Kurt Schlacher. Energy-based nonlinear Control of Hydraulically actuated Mechanical Systems. In *Proceedings of the 44<sup>th</sup> IEEE Conference on Decision and Control, and the European Control Conference 2005, Seville, Spain*, pages 7520–7525, 2005.
- [32] Helmut Kogler. *The Hydraulic Buck Converter - Conceptual Study and Experiments*. PhD thesis, Johannes Kepler University, Linz, Austria, 2012.
- [33] Bernd Winkler, Karl Ladner, Helmut Kogler, and Rudolf Scheidl. Switching Control of a Linear Hydraulic Drive - Experimental analysis. In *Proceedings of the 9<sup>th</sup> Scandinavian International Conference on Fluid Power, Linköping, Sweden*, 2005.
- [34] Helmut Kogler and Rudolf Scheidl. Energy Efficient Linear Drive Axis using a Hydraulic Switching Converter. *Journal of Dynamic Systems, Measurement, and Control*, 138(9), September 2016.
- [35] Arjan van der Schaft. *L<sub>2</sub>-Gain and Passivity Techniques in Nonlinear Control*. Springer London, 2000.
- [36] Donald M. Wiberg. *Schaum's Outline of Theory and Problems of State Space and Linear Systems*. McGRAW-HILL Book Company, 1971.
- [37] Alessandro Astolfi and Lorenzo Marconi. *Analysis and Design of Nonlinear Control Systems*. Springer, 2007.
- [38] Ingo Schepers, David Schmitz, Daniel Weiler, Olaf Cochoy, and Uwe Neumann. A Novel Model for Optimized Development and Application of Switching Valves in Closed Loop Control. *International Journal of Fluid Power*, 12(3):31–40, jan 2011.

**List of Figures**

- 1 Digital Hydraulic Concepts . . . . . 3
- 2 Hydraulic single acting ram (SAR) . 3
- 3 Single acting ram using a gas loaded accumulator for pressure attenuation (SAR) . . . . . 3
- 4 Gas-loaded accumulator; left: empty; right: fluid, respectively, energy is stored . . . . . 4
- 5 Block Scheme of the Interconnection and Damping Assignment Passivity Based Control (IDA-PBC) . . . . . 8
- 6 Simulation results . . . . . 9
- 7 Simulation results . . . . . 9

**List of Tables**

- 1 Exemplary parameters of a common linear hydraulic drive . . . . . 3